Z. Kristallogr. Suppl. **26** (2007) 247-252

Study of crystallization of magnetron sputtered TiO_2 thin films by X-ray scattering

R. Kužel[1*], L. Nichtová[1], Z. Matěj[2], D. Heřman[2], J. Šícha[2], J. Musil[2]

[1]Department of Condensed Matter Physics, Faculty of Mathematics and Physics, Charles University in Prague, Ke Karlovu 5, 121 16 Praha 2, Czech Republic;
[2]Department of Physics, Faculty of Applied Sciences, University of West Bohemia, P.O. Box 314, 306 14 Plzeň, Czech Republic
[*]Contact author; e-mail: kuzel@karlov.mff.cuni.cz.

Keywords: titanium oxide, crystallization, X-ray diffraction, thin films

Abstract. Crystallization of a set of magnetron deposited TiO_2 thin films with different thickness in the range of 54 – 2000 nm has been studied by X-ray scattering. Phase analysis, lattice parameters and X-ray line broadening were studied by X-ray powder diffraction in parallel beam optics, the residual stresses were measured with the aid of the Eulerian cradle and surface roughness determined by X-ray reflectivity measurement. As-deposited films were amorphous. They were annealed at different temperatures and found to be crystalline after annealing at 250 ºC except the thinnest films which crystallized at higher temperatures.

Introduction

In recent years, titanium dioxide films have been widely used in various fields because of their excellent chemical stability, mechanical hardness and optical transmittance with high refractive index. They have found various applications in the field of optical coatings [1], electronic devices [2], or protective layers [3]. Many researchers have focused on the application of TiO_2 photocatalyst to purification and treatment of air and water, e.g. through the photolysis of organics and toxic gases.

It is known that titanium dioxide belongs to the class of semiconductors with a relatively wide band gap. If it is exposed to light of energy corresponding to its band gap, electrons in the conduction band and holes in the valence band are produced. The generation of these carriers leads to oxidation and reduction reactions on the TiO_2 surface; therefore titanium dioxide is a very attractive material for applications in photocatalysis [4-6]. The photocatalytic activity of TiO_2 can result in the decomposition of organic compounds on the TiO_2 surface or the reduction of the contact angle between water and the TiO_2 surface under ultraviolet irradiation, i.e., in selfcleaning and antifogging effects, respectively.

Because of these outstanding activities, TiO_2 photocatalysts have been applied in various fields, in which the anti-fogging and self-cleaning activities should be quite attractive for the application for architectural or automobile windows.

TiO_2 can occur in 3 crystalline phases including tetragonal rutile ($P4_2/mnm$, a = 4.593 Å, c = 2.951 Å) and anatase ($I4_1/amd$, a = 3.784 Å, c = 9.515 Å) and orthorombic brookite (*Pbca*, a = 9.179 Å, b = 5.449 Å, c = 5.138 Å). Anatase possesses a higher photocatalytic activity than rutile due to the difference in the band gap (rutile 3.0 eV versus anatase 3.2 eV [7]).

At present, TiO_2 thin films for the photocatalytic applications are mainly produced by sol–gel processes [4, 6] but also by chemical vapor deposition [8, 9], evaporation [10], various sputtering depositions [11-13], and ion beam-assisted processes [14].

Sputtering methods are widely used in industrial products because the high quality films; high density, high adhesion, high hardness, etc., can be obtained at low substrate temperature with good uniformity of the film thickness in a large area. Unfortunately, the photocatalytic activity of the sputtered film used for architectural glass is lower than that of the films prepared by the wet process. Magnetron sputtering is a nonequilibrium process and many external deposition and internal plasma parameters can influence the film characteristics, such as the phase and chemical composition, the microstructure, and the surface morphology. The films deposited by magnetron sputtering at low temperatures are usually amorphous. In order to obtain crystalline form, it is necessary either to heat the films or to use higher deposition temperature. However, both is very inconvenient for practical use.

Studies of different sets of TiO_2 films are described in [15]. In the present work, the deposited amorphous films were annealed at different temperatures and their structure was studied by X-ray diffraction.

Experimental

A complex XRD study was performed on as-deposited amorphous TiO_2 films sputtered by dual magnetron and post-annealed at different annealing temperatures T_a. The magnetron was equipped with two Ti(99.5) targets of 50 mm in diameter and supplied by a dc–pulsed Advanced Energy Pinnacle Plus+ 5kW power supply unit (PSU) operating in bipolar asymmetric mode at repetition frequency f_r = 100 kHz and duty cycle τ/T = 0.5; here τ and T are the length of pulse and the period of pulses. Films were deposited on unheated microscope glass slides (26 × 26 × 1 mm^3) at substrate to target distance $d_{s\text{-}t}$ = 100mm, average pulse discharge current $I_{da1,2}$ = 1.5 A and average pulse power density W_{da} = 20 Wcm^{-2}. Depositions were performed in the transition mode of sputtering at oxygen partial pressure p_{O2} = 0.03 Pa, total working pressure p_T = 0.5 Pa and deposition rate a_D = 23 nm/min. Further details on dual magnetron system are given elsewhere [16].

Amorphous films with different thickness in the interval of 54 nm to 2000 nm were investigated after deposition and then after isochronal annealing at temperatures up to 500 °C (step - 50 °C, time - 0.5 hour) in the air in atmospheric pressure. The measurement was performed on two diffractometers - XRD7 (FPM-Seifert) and Philips X'Pert MRD in parallel beam setup, 2θ scans with angles of incidence 1-3° with parallel plate collimator placed in the diffracted beam and the Goebel mirror inserted in the primary beam (Philips). Phase analysis, lattice parameters and X-ray line profile analysis were studied. Detailed measurement of residual stresses was carried out on the Eulerian cradle by the $\sin^2\psi$ method for several peaks. In addition, X-ray reflectivity curves were measured for all the samples after annealing at each temperature. Methods have been partially described e.g. in [17].

Results

All the films studied remained amorphous up to the annealing temperature of 200 °C. After annealing at 250 °C in most of the samples the diffraction peaks of anatase phase have appeared except two thinnest layers (100 nm and 54 nm) which have shown indications of diffraction peaks only after annealing at 300 °C and 350 °C, respectively (see figures 1, 2).

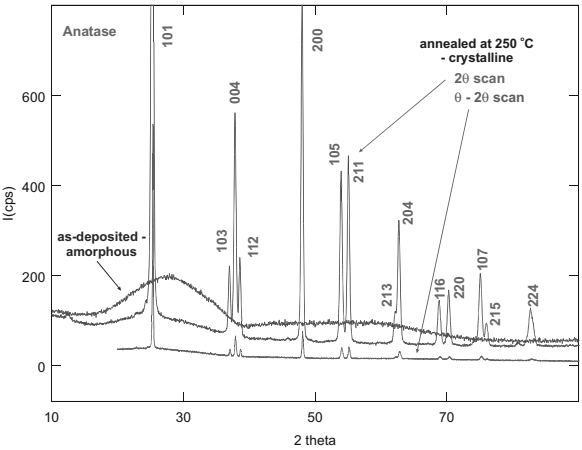

Figure 1. Diffraction patterns, 2θ scans, angle of incidence ω = 1.5°, of TiO_2 film with the thickness of 600 nm – as-deposited (broad maximum), after annealing at 250 ºC (with distinct sharp maxima corresponding to anatase, upper curve). The lower curve corresponds to the symmetrical θ-2θ scan for the same sample after annealing. The latter method, inconvenient for thin films because of larger penetration depth, is used mainly for the estimation of texture as it gives information only from the planes parallel to the surface.

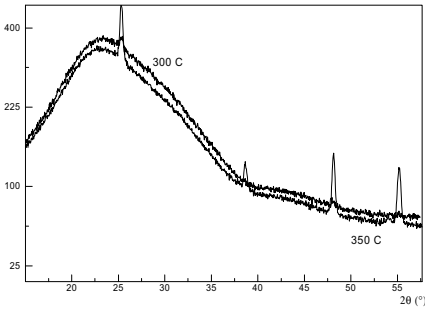

Figure 2. 2θ scans (ω = 1.5°) of TiO_2 film with the thickness of 100 nm – after annealing at 300 ºC (thick upper line with a small maximum at 26º) and 350 ºC (thin bottom line with clear maxima).

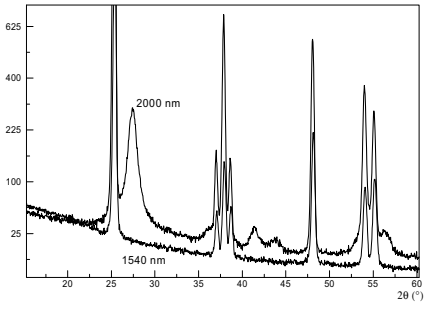

Figure 3. 2θ scans (ω = 1.5°) of TiO_2 film with the thickness of 2000 nm (upper line with clear broad maxima of rutile 110 at 27º) and 1540 nm (bottom line).

Diffraction patterns show pure anatase for thinner films and anatase with a small amount of rutile for thicker films (figure 3). However, the amount of rutile is not increasing monotonously. With further annealing above crystallization temperatures neither changes in peak intensities nor shapes have been observed which indicates no significant changes in texture, strain and crystallite size. *XRD line profile analysis* has shown that the line broadening of annealed films is caused mainly by strain (figure 4). The differences between samples are within the error limit for most of the samples except the thinnest ones and the values were not essentially changed after subsequent annealing up to 500 ºC.
Only weak textures of fiber type were detected in the films. For thinner films preferred orientation of the (101) type was found while for thicker films it goes more to (001) as estimated from the texture indices obtained from the symmetrical $\theta - 2\theta$ scans.

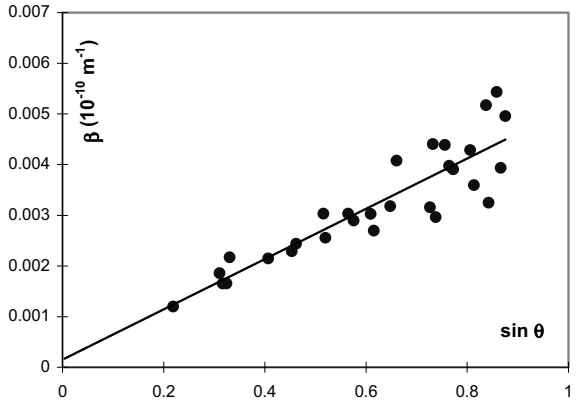

Thickness (nm)	Strain (%)	Size (nm)
400	0.144	130
630	0.144	130
800	0.179	250
1000	0.188	> 300
1200	0.191	> 300
1540	0.184	> 300
1700	0.170	> 300
2000	0.180	> 300

Figure 4. Typical Williamson-Hall plot (shown for the sample of the thickness h = 800 nm after annealing at 300 ºC), β is the integral breadth. The slope is proportional to microstrain, the reciprocal value of the intercept to the mean crystallite size. In the table, the values of microstrain and crystallite size are shown for different samples after annealing at 300 ºC. The values of the latter are on the sensitivity limit of the method.

X-ray reflectivity curves for thicker films had to be fitted with a two-layer model (commercial software by Panalytical) since no good agreement with a single layer model could be achieved. Very thin film, probably on the surface, can correspond to surface porous layer. An increase of the surface roughness with increasing film thickness was observed (figure 5). As expected, the roughness increased after crystallization of the films and it was increasing after next annealing up to 500 ºC as well. Very thin layer causing the long-period oscillations was systematically reduced with annealing temperature.
Residual stress measurements by the $\sin^2\psi$ method revealed linear dependences with positive slopes for all 8 measured peaks of anatase. This indicates the presence of simple tensile uniaxial stress in all the samples. For all crystalline films the stress of hundreds of MPa was found (figure 6). Systematic strong strain anisotropy was detected. However, it could not be explained by using the single-crystal elastic constants for rutile at all and unfortunately no

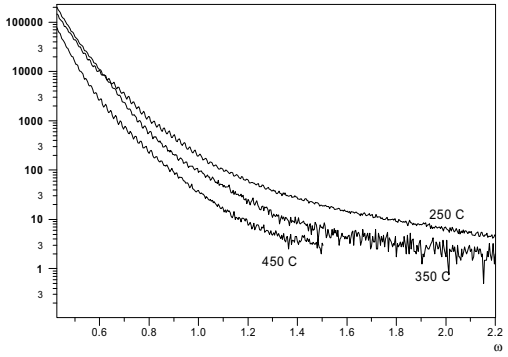

h (nm)	h_{fit} (nm)	ρ_{el} ($g.cm^{-3}$)	σ_r (nm)
54	57	3.42	1.2
100	93	3.58	1.7
200	200	3.48	1.8
630	570	3.53	4.1
	57	3.64	7
1000	970	3.89	2
	49	3.68	5
1700	1790	3.89	2
	55	3.74	5

Figure 5. Left - reflectivity curves for the film 200 nm thick after annealing at 250, 350 and 450 °C, respectively from the top. Faster decrease of the reflectivity curves with annealing temperature indicates increasing roughness. Right – table of the fitted values of film thickness h_{fit}, electron density ρ_{el} and surface roughness σ_r are shown.

data on these constants for anatase was found in the literature. Therefore, the stress was only evaluated by using isotropic Young modulus and Poisson ratio. With increasing annealing temperature the stress is reduced and after annealing at 500 °C it dropped down to zero except for the thinnest films. Higher stress values were also found in thinnest films.

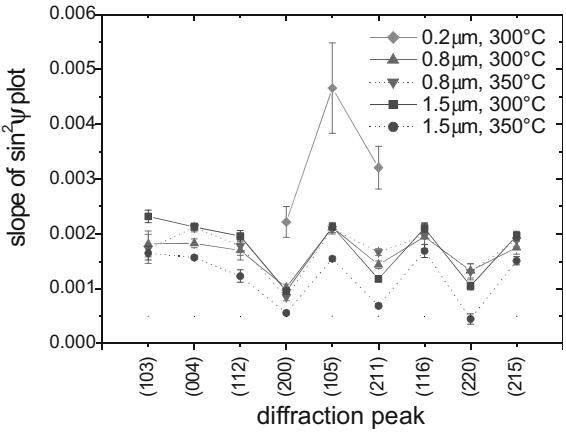

h (nm)	σ(Mpa)		
	300 °C	350 °C	500 °C
200		341	151
630	187	187	42
800	219	209	0
1000	184	154	0
1500	240	163	0
1700	280	232	0
2000	293	252	0

Figure 6. Left - slopes of $sin^2\psi$ plots for different peaks and samples showing characteristic anisotropy. Right – average stress values determined from the $sin^2\psi$ plots for 9 diffraction peaks and using isotropic elastic moduli. Values for three annealing temperatures are shown.

Summary

Magnetron sputtered amorphous TiO_2 films can be crystallized at approximately 250 °C. Their crystallite size is then immediately above 100 nm. This is very different from as-deposited nanocrystalline films (~ 5 nm) which do not change after annealing in this temperature range [18]. The films with the thickness below 400 nm crystallize at higher temperatures (350 °C). Diffraction patterns do not change significantly after annealing up to 600 °C. Tensile residual stresses have been found in crystallized films. They relaxed after annealing at 500 °C. Fiber texture is usually not very strong and of the 100 type for thicker films (above 1500 nm) and 101 for thinner films. Surface roughness increases with the increasing annealing temperature as well as the increasing film thickness.

References

1. Suhail, M.H., Mohan Rao, G. & Mohan, S., 1992, *J. Appl. Phys.*, **71**, 1421.
2. Tang, H., Prasad, K., Sanjines, R., Schmid, P.E. & Levy, F., 1994, *J. Appl. Phys.*, **75**, 2042.
3. Perry, A.J. & Pulker, H.K., 1985, *Thin Solid Films*, **124**, 323.
4. Sopyan, N., Watanabe, M., Murasawa, S., Hashimoto, K. & Fujishima, A., 1996, *J. Photochem. Photobiol.*, **A98**, 79.
5. Byun, I., Jin, Y., Kim, B., Lee, J.K. & Park, D., 2000, *J. Haz. Mat.*, **B73**, 199.
6. Negishi, J., Takeuchi, M. & Ibusuki, T., 1998, *J. Mater. Sci.*, **33**, 5789.
7. Mills, A. & Le Hunte, S., 1997, *J. Photochem. Photobiol.*, **A108** 1.
8. Battiston, G.A., Gerbasi, R., Porchia, M. & Marigo, A., 1994, *Thin Solid Films*, **239**, 186.
9. Williams, L.M. & Hess, D.W., 1983, *J. Vac. Sci. Technol.*, **A1**, 1810.
10. Fujii, T., Sakata, N., Takada, J., Miura, Y. & Daitoh, Y., 1994, *J. Mater. Res.*, **9** (6), 1468.
11. Tang, H., Prasad, K., Sanjines, R., Schmid, P.E. & Levy, F.,1994, *J. Appl. Phys.*, **75**, 2042.
12. Ben Amor, S., Baud, G., Besse, J.P. & Jacqet, M., 1997, *Thin Solid Films*, **293**, 163.
13. Martin, N., Rousselot, C., Rondot, D. & Palmino, F., 1997, *Thin Solid Films*, **300**, 113.
14. Gilo, M. & Croitoru, N., 1996, *Thin Solid Films*, **283**, 84.
15. J. Musil, D. Heřman, J. Šícha, 2006, *J. Vac. Sci. Technol.*, **A24** (3), 521.
16. Baroch, P., Musil, J., Vlcek, J., Nam, K.H. & Han, J.G., 2005, *Surf. Coat. Technol.*, **193**, 107.
17. Kužel, Jr., R., Černý, R., Valvoda, V., Blomberg, M. & Merisalo, M., 1994, *Thin Solid Films*, **247**, 64.
18. Kužel, R., Nichtová, L., Matěj, Z., Šícha, J. & Musil, J., in preparation.

Acknowledgements. The work is supported by the Grant Agency of the Czech Republic under number 106/06/0327 and also as a part of the research plans MSM 0021620834 and MSM 4977751302 financed by the Ministry of Education of the Czech Republic.